

# Contents

<b>Summary</b>	<b>ii</b>
<b>Introduction</b>	<b>1</b>
Human Mesenchymal Stem/Stromal Cells . . . . .	2
Multiple Myeloma . . . . .	3
Myeloma-hMSC Interactions . . . . .	3
Myeloma Bone Disease . . . . .	3
Dissemination of Myeloma Cells . . . . .	4
Code-Automation as a Standard in Modern Biosciences . . . . .	5
How Code Quality Improves Scientific Reproducibility . . . . .	6
Python as a Programming Language . . . . .	8
Data Science with Python . . . . .	12
Aims . . . . .	14
<b>Chapter 1: Modelling Myeloma Dissemination <i>in vitro</i></b>	<b>15</b>
Abstract . . . . .	15
Introduction . . . . .	16
Materials and Methods . . . . .	18
Results . . . . .	22
Discussion . . . . .	34
<b>Chapter 2: Semi-Automating Data Analysis with <code>plotastic</code></b>	<b>35</b>
Abstract . . . . .	35
Introduction . . . . .	36
Statement of Need . . . . .	38
Example . . . . .	39
Overview . . . . .	41
Discussion . . . . .	43
<b>Summarising Discussion</b>	<b>45</b>
Time Lapse . . . . .	45
Myeloma . . . . .	45
Semi-Automated Analysis Improves Agility During Establishing new <i>in vitro</i> Methods . . . . .	45
<b>References</b>	<b>46</b>
<b>Appendices</b>	<b>54</b>
<b>A Supplementary Data &amp; Methods</b>	<b>54</b>
A.1 Figures . . . . .	54
A.2 Tables . . . . .	71
A.3 Materials & Methods . . . . .	79
<b>B Documentation of <code>plotastic</code></b>	<b>96</b>
B.1 Class Diagram . . . . .	97
B.2 Readme . . . . .	99
B.3 Example Analysis “qpcr” . . . . .	112
<b>C Submission Forms &amp; Documents</b>	<b>119</b>

## Contents

---

C.1	Author Contributions . . . . .	119
C.2	Affidavit . . . . .	126
C.3	Curriculum Vitae . . . . .	128

## **Introduction**

To provide a comprehensive background for the following chapters that focus on the interaction of human mesenchymal stromal cells (hMSCs) with multiple myeloma (MM) cells, this

## Aims

This project defines these aims:

- Characterize the interaction between myeloma cells and mesenchymal stromal cells
- Aim 2
- Aim 3

# Chapter 1: Modelling Myeloma Dissemination *in vitro*

## Abstract

Multiple myeloma involves early dissemination of malignant plasma cells across the bone marrow; however, the initial steps of dissemination remain unclear. Human bone marrow-derived mesenchymal stromal cells (hMSCs) stimulate myeloma cell expansion (e.g., IL-6) and simultaneously retain myeloma cells via chemokines (e.g., CXCL12) and adhesion factors. Hence, we hypothesized that the imbalance between cell division and retention drives dissemination. We present an *in vitro* model using primary hMSCs co-cultured with INA-6 myeloma cells. Time-lapse microscopy revealed proliferation and attachment/detachment dynamics. Separation techniques (V-well adhesion assay and well plate sandwich centrifugation) were established to isolate MSC-interacting myeloma sub-populations that were characterized by RNAseq, cell viability and apoptosis. Results were correlated with gene expression data ( $n = 837$ ) and survival of myeloma patients ( $n = 536$ ). On dispersed hMSCs, INA-6 saturate hMSC-surface before proliferating into large homotypic aggregates, from which single cells detached completely. On confluent hMSCs, aggregates were replaced by strong heterotypic hMSC-INA-6 interactions, which modulated apoptosis time-dependently. Only INA-6 daughter cells (nMA-INA6) detached from hMSCs by cell division but sustained adherence to hMSC-adhering mother cells (MA-INA6). Isolated nMA-INA6 indicated hMSC-autonomy through superior viability after IL-6 withdrawal and upregulation of proliferation-related genes. MA-INA6 upregulated adhesion and retention factors (CXCL12), that, intriguingly, were highly expressed in myeloma samples from patients with longer overall and progression-free survival, but their expression decreased in relapsed myeloma samples. Altogether, *in vitro* dissemination of INA-6 is driven by detaching daughter cells after a cycle of hMSC-(re)attachment and proliferation, involving adhesion factors that represent a bone marrow-retentive phenotype with potential clinical relevance.

## Statement of Significance

Novel methods describe *in vitro* dissemination of myeloma cells as detachment of daughter cells after cell division. Myeloma adhesion genes were identified that counteract *in vitro* detachment with potential clinical relevance.

## Introduction

Multiple myeloma arises from clonal expansion of malignant plasma cells in the bone marrow (BM). At diagnosis, myeloma cells have disseminated to multiple sites in the skeleton and, in some cases, to “virtually any tissue” (Bladé et al., 2022; Rajkumar et al., 2014). However, the mechanism through which myeloma cells initially disseminate remains unclear. Dissemination is a multistep process involving invasion, intravasation, intravascular arrest, extravasation, and colonization (Zeissig et al., 2020). To initiate dissemination, myeloma cells overcome adhesion, retention, and dependency on the BM microenvironment, which could involve the loss of adhesion factors such as CD138 (Akhmetzyanova et al., 2020; García-Ortiz et al., 2021). BM retention is mediated by multiple factors: First, chemokines (CXCL12 and CXCL8) produced by mesenchymal stromal cells (MSCs), which attract plasma cells and prime their cytoskeleton and integrins for adhesion (Aggarwal et al., 2006; Alsayed et al., 2007). Second, myeloma cells must overcome the anchorage and physical boundaries of the extracellular matrix (ECM), consisting of e.g. fibronectin, collagens, and proteoglycans such as decorin (Hu et al., 2021; Huang et al., 2015; Katz, 2010; Kibler et al., 1998). Simultaneously, ECM provides signals inducing myeloma cell cycle arrest or progression the cell cycle (Hu et al., 2021; Katz, 2010). ECM is also prone to degradation, which is common in several osteotropic cancers, and is the cause of osteolytic bone disease. This is driven by a ‘vicious cycle’ that maximizes bone destruction by extracting growth factors (EGF and TGF- $\beta$ ) that are stored in calcified tissues (Glavey et al., 2017). Third, direct contact with MSCs physically anchors myeloma cells to the BM (Zeissig et al., 2020; Sanz-Rodríguez et al., 1999). Fourth, to disseminate to distant sites, myeloma cells require, at least partially, independence from essential growth and survival signals provided by MSCs in the form of soluble factors or cell adhesion signaling (García-Ortiz et al., 2021; Chatterjee et al., 2002; Hideshima et al., 2007). For example, the VLA4 (Myeloma)-VCAM1 (MSC)-interface activates NF- $\kappa$ B in both myeloma and MSCs, inducing IL-6 expression in MSCs. The independence from MSCs is then acquired through autocrine survival signaling (Frassanito et al., 2001; Urashima et al., 1995). In short, anchorage of myeloma cells to MSCs or ECM is a ‘double-edged sword’: adhesion counteracts dissemination, but also presents signaling cues for growth, survival, and drug resistance (Solimando et al., 2022).

To address this ambiguity, we developed an *in vitro* co-culture system modeling diverse adhesion modalities to study dissemination, growth, and survival of myeloma cells and hMSCs. Co-cultures of hMSCs and the myeloma cell line INA-6 replicated tight interactions and aggregate growth, akin to “micrometastases” in Ghobrial’s metastasis concept (Ghobrial, 2012). We characterized the growth conformations of hMSCs and INA-6 as homotypic aggregation *vs.* heterotypic hMSC adherence and their effects on myeloma cell survival. We tracked INA-6 detachments from aggregates and hMSCs, thereby identifying a potential “disseminated” sub-

population lacking strong adhesion. We developed innovative techniques (V-well adhesion assay and well plate sandwich centrifugation) to separate weakly and strongly adherent subpopulations for the subsequent analysis of differential gene expression and cell survival. Notably, our strategy resolves the differences in gene expression and growth behavior between cells of one cell population in “direct” contact with MSCs. In contrast, previous methods differentiated between “direct” and “indirect” cell-cell contact using transwell inserts (Dziadowicz et al., 2022). To evaluate whether genes mediating adhesion and growth characteristics of INA-6 were associated with patient survival, we analyzed publicly available datasets (Seckinger et al., 2017, 2018).

## Materials and Methods

See Appendix A.3 for a complete method list and description.

### Ethics Statement

Primary human MSCs were collected with the written informed consent of all patients. The procedure was conducted in accordance with recognized ethical guidelines (Helsinki Declaration) and approved by the local Ethics Committee of the University of Würzburg (186/18).

### Cultivation and Co-Culturing of primary hMSCs and INA-6

Primary human MSCs were obtained from the femoral head of 34 non-myeloma patients (Appendix A: Table 1: 21 male and 13 female, mean age  $68.9 \pm 10.6$ ) undergoing elective hip arthroplasty. The INA-6 cell line (*DSMZ Cat# ACC-862, RRID:CVCL\_5209*, link) was initially isolated from a pleural effusion sample obtained from an 80-year-old male with multiple myeloma (Burger, Günther, et al., 2001; Gramatzki et al., 1994). hMSCs were not tested for mycoplasma, whereas stocks of INA-6 were tested in this study (Appendix A: Table 1) using the *Venor GEM OneStep* kit (Minerva Biolabs, Berlin, Germany). For each co-culture, hMSCs were seeded 24 h before INA-6 addition to generate the MSC-conditioned medium (CM). INA-6 cells were washed with PBS, resuspended in MSC medium, and added to hMSCs so that the co-culture comprised 33 % (v/v) of CM gathered directly from the respective hMSC donor. The co-cultures were not substituted for IL-6 (Chatterjee et al., 2002).

### Cell Viability and Apoptosis Assay

Cell viability and apoptosis rates were measured using *CellTiter-Glo Luminescent Cell Viability Assay* and *Caspase-Glo 3/7 Assay*, respectively (Promega GmbH, Mannheim, Germany).

### Automated Fluorescence Microscopy

Microscopic images were acquired using an Axio Observer 7 (Zeiss) with a COLIBRI LED light source and motorized stage top using 5x and 10x magnification. The tiled images had an automatic 8–10 % overlap and were not stitched.

## Live Cell Imaging

hMSCs (stained with PKH26) were placed into an ibidi Stage Top Incubation System and equilibrated to 80 % humidity and 5 % CO<sub>2</sub>. INA-6 ( $2 \times 10^3$  cells/cm<sup>2</sup>) were added directly before the start of acquisition. Brightfield and fluorescence images of up to 13 mm<sup>2</sup> of the co-culture area were acquired every 15 min for 63 h. Each event of interest was manually analyzed and categorized into defined event parameters.

## V-well Adhesion Assay

INA-6 cells were arrested during mitosis by two treatments with thymidine, followed by nocodazole. Arrested INA-6 were released and added to 96 V-well plates (10<sup>4</sup> cells/cm<sup>2</sup>) on top of confluent hMSCs and adhered for 1–3 h. The co-culture was stained with calcein-AM (Thermo Fisher Scientific, Darmstadt, Germany) before non-adherent INA-6 were pelleted into the tip of the V-well (2000 rpm, 5–10 min). MSC-adhering INA-6 cells were manually detached by rapid pipetting. The pellet brightness was measured microscopically and the pellet was isolated by pipetting.

## Cell Cycle Profiling by Image Cytometry

Isolated INA-6 cells were fixed in 70 % ice-cold ethanol, washed, resuspended in PBS, distributed in 96-well plates, and stained with Hoechst 33342. The plates were scanned at 5x magnification. A pre-trained convolutional neural network (Intellesis, Zeiss) was fine-tuned to segment the scans into single nuclei and exclude fragmented nuclei. Nuclei were filtered to exclude extremes of size and roundness. The G0/G1 frequency was determined by Gaussian curve fitting.

## Well Plate Sandwich Centrifugation (WPSC)

hMSCs were grown to confluence in 96-well plates coated with collagen I (rat tail; Corning, NY, USA). INA-6 cells were added and the cells were allowed to adhere for 24 h. A second plate (“catching plate”) was attached upside down to the top of the co-culture plate. That “well plate sandwich” was turned around and the content of the co-culture plate was centrifuged into the catching plate three times (40 s at 110 g) while gently adding 30 µL of medium in between centrifugation steps. Non-MSC-adhering INA-6 cells were collected from the catching plate, whereas MSC-adhering INA-6 cells were isolated by digesting the co-culture with accutase. For RNA sequencing (RNAseq), all samples were purified using anti-CD45 magnetic-assisted cell sorting (Miltenyi Biotec B.V. & Co. KG, Bergisch Gladbach).

## RNA Isolation

RNA was isolated using the *NucleoSpin RNA II Purification Kit* (Macherey-Nagel) according to the manufacturer's instructions. RNA was isolated from INA-6 cells co-cultured with a unique hMSC donor ( $n = 5$  for qPCR,  $n = 11$  for RNA sequencing).

## RNA sequencing, Differential Expression, and Functional Enrichment Analysis

RNA sequencing (RNAseq) was performed at the Core Unit Systems Medicine, University of Würzburg. mRNA was enriched with polyA beads. Fastq files were aligned to the GRCh38 reference genome using STAR (*RRID:SCR\_004463*, link) and raw read counts were generated using HTseq (*RRID:SCR\_005514*, link) (Anders et al., 2015; Dobin et al., 2013; Zerbino et al., 2018). Differential gene expression was analyzed using edgeR in R (version 3.6.3) (*RRID:SCR\_012802*, link). Functional enrichment analysis was performed using Metascape (*RRID:SCR\_016620*, link) (Zhou et al., 2019).

## RT-qPCR

RNA ( $1\ \mu\text{g}$ ) was reverse transcribed using *SuperScript IV reverse transcriptase* (Thermo Fisher Scientific). qPCR was performed using  $10\ \mu\text{L}$  *GoTaq qPCR Master Mix* (Promega), 1:10 diluted cDNA, and 5 pmol of primers obtained from Biomers.net or Qiagen (Appendix A: Table 3).

## Statistics

Inferential statistics were performed using Python (IPython, *RRID:SCR\_001658*, link) (3.10) packages *pingouin* (0.5.1) and *statsmodels* (0.14.0) (Vallat, 2018; Seabold & Perktold, 2010). The figures were plotted using *plotastic* (0.0.1) (Kuric & Ebert, 2024). Normality (for  $n \geq 4$ ) and sphericity were ensured using Mauchly's and Shapiro-Wilk tests, respectively. Data points were  $\log_{10}$  transformed to convert the scale from multiplicative to additive or to fulfill sphericity requirements.  $p = 0.05 > * > 0.01 > ** > 10^{-3} > *** > 10^{-4} > ****$ . p-values were either adjusted (p-adj) or not adjusted (p-unc) for family wise error rate. Power calculations were not performed to determine the sample size.

## Patient Cohort, Analysis of Survival and Expression

Survival and gene expression data were obtained as previously described (Seckinger et al., 2017, 2018) and are available at the European Nucleotide Archive (ENA) under accession numbers

PRJEB36223 and PRJEB37100. The expression level was categorized into “high” and “low” using maxstat (Maximally selected Rank Statistics) thresholds (Hothorn & Lausen, n.d.).

## Data Availability Statement

A detailed description of the methods is provided in the Supplementary Material section. Raw tabular data and examples of analyses and videos are available in the github repository, [link](#). Raw RNAseq data are available from the NCBI Gene Expression Omnibus (GEO) (*RRID:SCR\_005012*, [link](#)) (GSE261423). Microscopy data are available at BioStudies (EMBL-EBI) (*RRID:SCR\_004727*, [link](#)) (S-BIAD1092).

## Results

### INA-6 Cells Saturate hMSC-Interaction to Proliferate into Aggregates

hMSCs are isolated as a heterogeneous cell population. To analyze whether INA-6 cells could adhere to every hMSC, we saturated hMSCs with INA-6. A seeding ratio of 1:4 (hMSC:INA-6) resulted in the occupation of  $93 \pm 6\%$  of single hMSCs by one or more INA-6 cells within 24 hours after INA-6 addition, escalating to 6% after 48 hours (Figure 1A, B). Therefore, most hMSCs provide an interacting surface for INA-6 cells.

INA-6 exhibits homotypic aggregation when cultured alone, a phenomenon observed in some freshly isolated myeloma samples (up to 100 cells after 6 hours) (Kawano et al., 1991; Okuno et al., 1991). Adding hMSCs at a 1:1 ratio led to smaller aggregates after 24 hours (size 1–5 cells), all of which were distributed over  $52 \pm 2\%$  of all hMSCs (Figure 1A, B). Intriguingly, INA-6 aggregation was notably absent when grown on confluent hMSCs, and occurred only when heterotypic interactions were limited to 0.2 hMSCs per INA-6 cell (Figure 1C). We concluded that INA-6 cells prioritize heterotypic over homotypic interactions.

To monitor the formation of such aggregates, we conducted live-cell imaging of hMSC/INA-6 co-cultures for 63 hours. We observed that INA-6 cells adhered long after cytokinesis, constituting  $55 \pm 12\%$  of all homotypic interactions between 13 hours and 26 hours, increasing to more than 75% for the remainder of the co-culture (Figure 1D). Therefore, homotypic INA-6 aggregates were mostly formed by cell division.

### Apoptosis of INA-6 Depends on Ratio Between Heterotypic and Homotypic Interaction

Although direct interaction with hMSCs has been shown to enhance myeloma cell survival through NF- $\kappa$ B signaling (Hideshima et al., 2007), the impact of aggregation on myeloma cell viability during hMSC interaction remains unclear. To address this, we measured the cell viability (ATP) and apoptosis rates of INA-6 cells growing as homotypic aggregates compared to those in heterotypic interactions with hMSCs by modulating hMSC density (Figure 1E). To equalize the background signaling caused by soluble MSC-derived factors, all cultures were incubated in hMSC-conditioned medium and the results were normalized to INA-6 cells cultured without direct hMSC contact (Figure 1E, left).

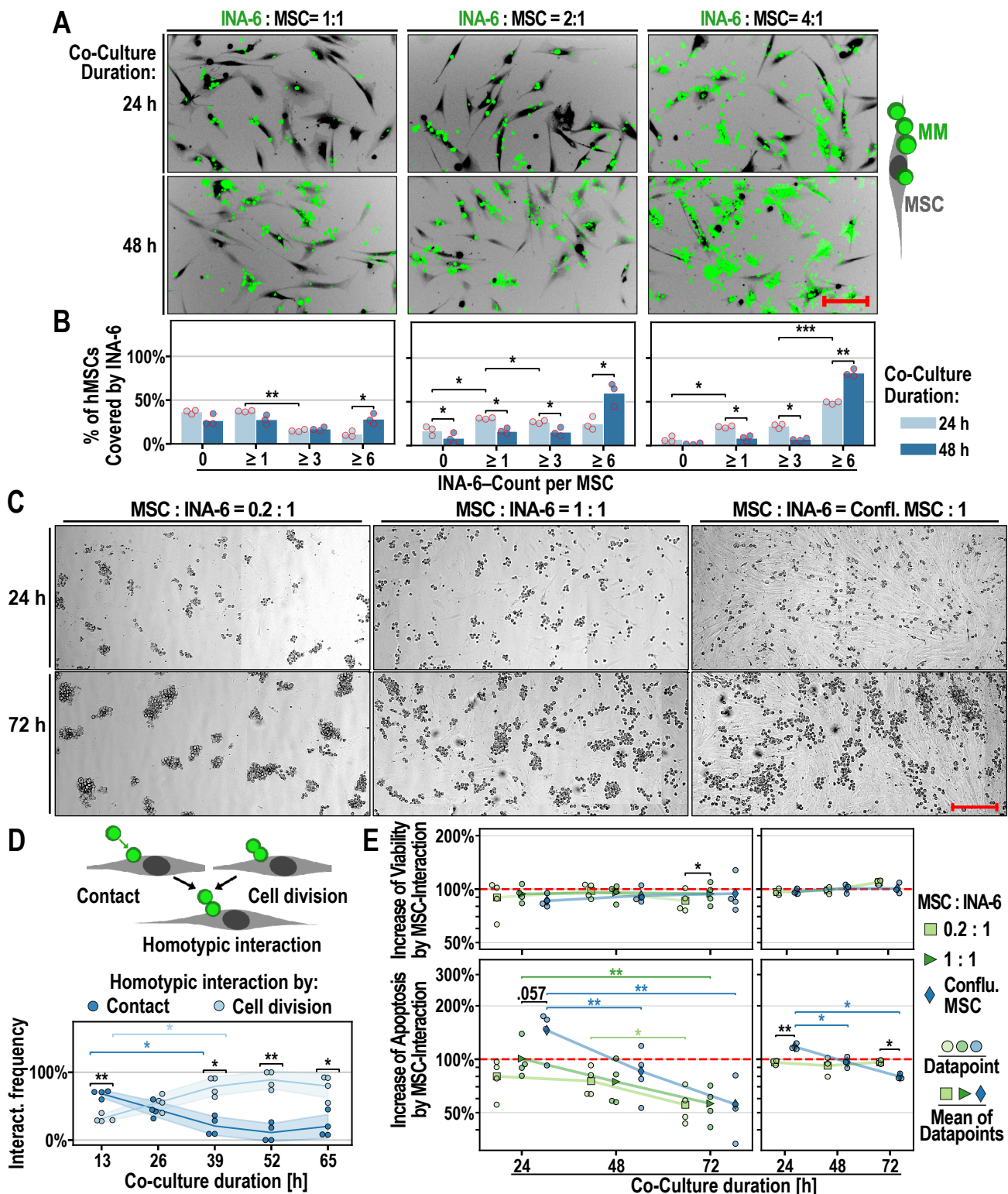


**Figure 1:** INA-6 growth conformations and survival on hMSCs. **A:** Interaction of INA-6 (green) with hMSCs (black, negative staining) at different INA-6 densities (constant hMSC densities). Scale bar = 200 μm. **B:** Frequency of single hMSCs (same as A) that are covered by INA-6 of varying group sizes. Technical replicates = three per datapoint; Single hMSCs evaluated: 100 per technical replicate. **C:** Interaction of INA-6 with hMSCs at different hMSC densities (constant INA-6 densities). Scale bar = 300 μm. – *Continued on next page*

*Continued from previous page –* **D:** Two types of homotypic interaction: Attachment after cell contact and sustained attachment of daughter cells after cell division. Datapoints represent one of four independent time-lapse recordings, each evaluating 116 interaction events. **E:** Effects of hMSC-density on the viability (ATP, top) and apoptosis (Caspase3/7 activity, bottom). INA-6:MSC ratio = 4:1; Technical replicates = four per datapoint; **E left:** Signals were measured in INA-6 washed off from hMSCs and normalized by INA-6 cultured in MSC-conditioned medium (= red line) ( $n = 4$ ). **E right:** Signals were measured in co-cultures and normalized by the sum of the signals measured in hMSC and INA-6 cultured separately (= red line) ( $n = 3$ ). **Statistics:** Paired t-test, two-factor RM-ANOVA. Datapoints represent independent co-cultures with hMSCs from three (A, B, D, E right), four (E left) unique donors. Confl. = Confluent.

INA-6 viability (ATP) was not affected by the direct adhesion of hMSCs at any density. However, apoptosis rates decreased over time [ $F(2, 6) = 23.29$ ,  $p\text{-unc} = 1.49 \times 10^{-3}$ ] (Two-factor RM-ANOVA), interacting significantly with MSC density [ $F(4, 12) = 6.98$ ,  $p\text{-unc} = 3.83 \times 10^{-3}$ ] For example, 24 hours of adhesion to confluent MSCs increased apoptosis rates by  $1.46 \pm 0.37$  fold, while culturing INA-6 cells on dispersed hMSCs (ratio 1:1) did not change the apoptosis rate ( $1.01 \pm 0.26$  fold).

We presumed that sensitive apoptotic cells might have been lost when harvesting INA-6 cells from hMSCs. Hence, we measured survival parameters in the co-culture and in hMSC and INA-6 cells cultured separately (Figure 1E, right). We defined MSC interaction effects when the survival measured in the co-culture differed from the sum of the signals measured from INA-6 and hMSCs alone. RM-ANOVA confirmed that adherence to confluent MSCs increased apoptosis rates of INA-6 cells 24 hours after adhesion and decreased after 72 hours [ $F(2, 4) = 26.86$ ,  $p\text{-unc} = 4.80 \times 10^{-3}$ ] (interaction between MSC density and time, Two-factor RM-ANOVA), whereas INA-6 cells were unaffected when grown on dispersed hMSCs.

In summary, the growth conformation of INA-6 cells, measured as the ratio between homotypic aggregation and heterotypic MSC interactions, affected apoptosis rates of INA-6 cells.

### Single INA-6 Cells Detach Spontaneously from Aggregates of Critical Size

Using time-lapse microscopy, we observed that  $26 \pm 8\%$  of INA-6 aggregates growing on single hMSCs spontaneously shed INA-6 cells (Figure 2A, B; Supplementary Video 1). Notably, all detached cells exhibited similar directional movements, suggesting entrainment in convective streams generated by temperature gradients within the incubation chamber. INA-6 predominantly detached from other INA-6 cells or aggregates (Figure 2C), indicating weaker adhesive forces in homotypic interactions than in heterotypic interactions. The detachment frequency increased after 52 hours, when most aggregates that shed INA-6 cells were categorized as large (greater than 30 cells) (Figure 2D). Since approximately 10-20 INA-6 cells already fully covered a single hMSC, we suggest that myeloma cell detachment depended not only on hMSC saturation but also required a minimum aggregate size. Interestingly, INA-6 detached mostly as single cells, independent of aggregate size categories [ $F(2, 6) = 4.68$ ,  $p\text{-unc} = 0.059$ ] (Two-factor

RM-ANOVA) (Figure 2E), showing that aggregates remained mostly stable despite losing cells.

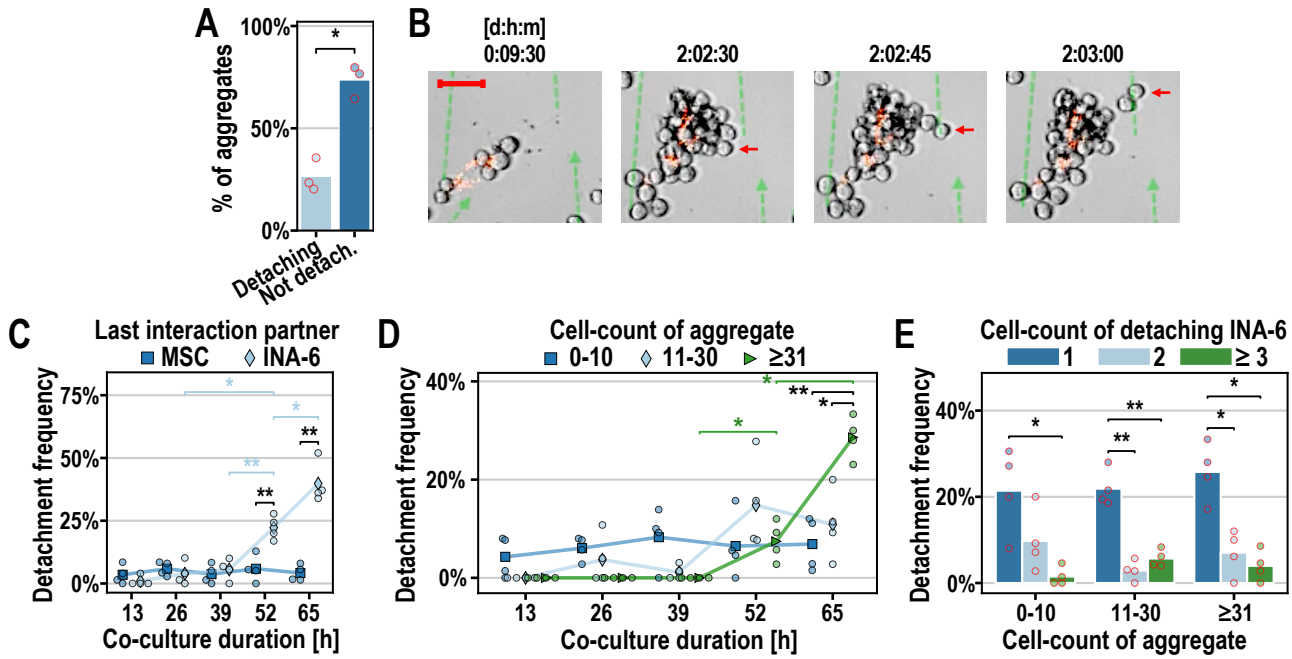


**Figure 2:** Time-lapse analysis of INA-6 detachment from INA-6 aggregates and hMSCs. **A:** Frequency of observed INA-6 aggregates that did or did not lose INA-6 cell(s). 87 aggregates were evaluated per datapoint. **B:** Example of a “disseminating” INA-6 aggregate growing on fluorescently (PKH26) stained hMSC (from A-D). Dashed green lines are trajectories of detached INA-6 cells. Scale bar = 50 µm. **C-E:** Quantitative assessment of INA-6 detachments. 45 detachment events were evaluated per datapoint. Seeding ratio INA-6:MSC = 4:1. **C:** Most INA-6 cells dissociated from another INA-6 cell and not from an hMSC [ $F(1, 3) = 298$ ,  $p\text{-unc} = 4.2 \times 10^{-4}$ ]. **D:** Detachment frequency of aggregate size categories. **E:** Detachment frequency of INA-6 cells detaching as single, pairs or more than three cells. **Statistics:** (A): Paired-t-test; (C-E): Paired-t-test, Two-factor RM-ANOVA; Datapoints represent three (A) or four (C-E) independent time-lapse recordings of co-cultures with hMSCs from two (A) or three (C-E) unique donors.

## Cell Division Generates a Daughter Cell Detached from hMSC

We suspected that cell division drives detachment because we observed that MSC-adhering INA-6 cells could generate daughter cells that “roll over” the mother cell (Figure 3A; Supplementary Video 2). We recorded and categorized the movement of INA-6 daughter cells in confluent hMSCs after cell division. Half of all INA-6 divisions yielded two daughter cells that remained stationary, indicating hMSC adherence (Figure 3B, C; Supplementary Video 3). The other half of division events generated one hMSC-adhering (MA-INA6) cell and one non-hMSC-adhering (nMA-INA6) cell, which rolled around the MA-INA6 cell for a median time of 2.5 hours post division ( $Q_1 = 1.00$  hour,  $Q_3 = 6.25$  hours) until it stopped and re-adhered to the hMSC monolayer (Figure 3D; Supplementary Video 2, Supplementary Video 4). Thus, cell division establishes a time window in which one daughter cell can detach.

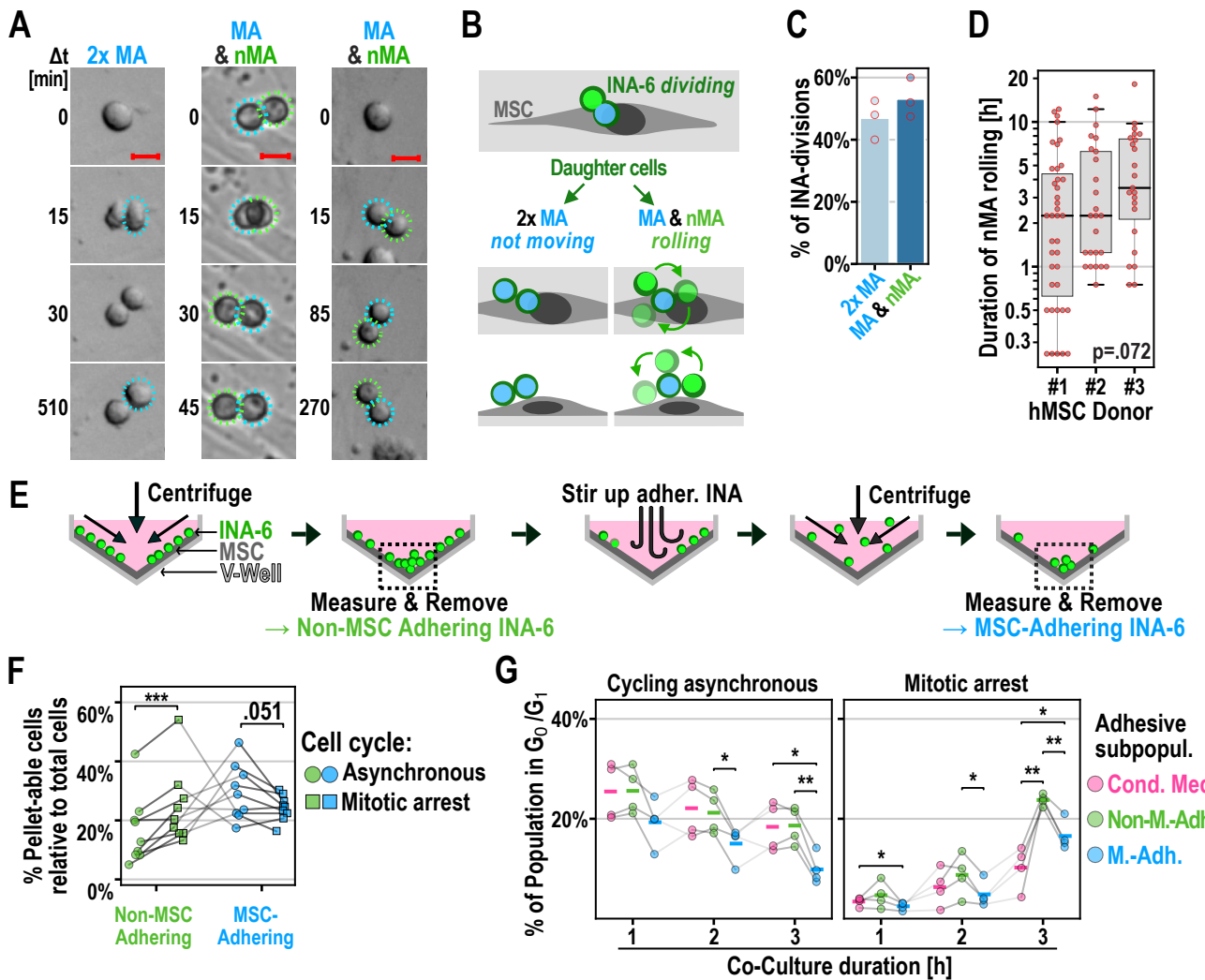


**Figure 3:** Detachment of INA-6 daughter cells after Cell Division. **A-D:** INA-6 divisions in interaction with confluent hMSCs. Seeding ratio INA-6:MSC = 4:20. **A:** Three examples of dividing INA-6 cells generating either two MA, or one MA and one nMA daughter cells as described in (G). Dashed circles mark mother cells (white), MA cell (blue), and first position of nMA cell (green). Scale bar: 20 µm. **B:** Cell division of MSC-adhering (MA) mother cell can yield one mobile non-MSC-adhering (nMA) daughter cell. **C:** Frequencies of INA-6 pairs defined in (A, B) per observed cell division. 65 divisions were evaluated for each of three independent time-lapse recordings. **D:** Rolling duration of nMA cells after division did not depend on hMSC donor [ $H(2) = 5.250$ ,  $p\text{-unc} = .072$ ]. Datapoints represent single nMA-cells after division. **E-G:** Adhesive and cell cycle assessment of MSC-interacting INA-6 subpopulations using the V-Well assay. **E:** Schematic of V-Well Assay (see Appendix A: Figure 1 for detailed analysis). MSC-interacting subpopulations were separated by subsequent centrifugation and removal of the pellet. The pellet size was quantified by its total fluorescence brightness. Adhering subpopulations were resuspended by rough pipetting. **F:** Relative cell pellet sizes of adhesive INA-6 subpopulations that cycle either asynchronously or were synchronized at mitosis. Gray lines in-between points connect dependent measurements of co-cultures ( $n = 9$ ) that shared the same hMSC-donor and INA-6 culture. Co-cultures were incubated for three different durations (1 h, 2 h and 3 h after INA-6 addition). Time points were pooled, since time did not show an effect on cell adhesion [ $F(2, 4) = 1.414$ ,  $p\text{-unc} = 0.343$ ] Factorial RM-ANOVA shows an interaction between cell cycle and the kind of adhesive subpopulation [ $F(1, 8) = 42.67$ ,  $p\text{-unc} = 1.82 \times 10^{-4}$ ]. Technical replicates = 4 per datapoint. **G:** Cell cycles were profiled in cells gathered from the pellets of four independent co-cultures ( $n = 4$ ) and the frequency of G<sub>0</sub>/G<sub>1</sub> cells are displayed depending on co-culture duration (see Appendix A: Figure 3 for cell cycle profiles). Four technical replicates were pooled after pelleting. **Statistics:** (D): Kruskal-Wallis H-test. (F): Paired t-test, (G): Paired t-test, two-factor RM-ANOVA. Datapoints represent INA-6 from independent co-cultures with hMSCs from three unique donors.

To validate that cell division reduced adhesion, we measured both the size and cell cycle profile of the nMA-INA6 and MA-INA6 populations using an enhanced V-well assay (method described in Figure 3E, Appendix A: Figure 1, 2). For comparison, we fully synchronized and arrested INA-6 cells at mitosis and released their cell cycle immediately before addition to the hMSC monolayer, rendering them more likely to divide while adhering. Mitotic arrest significantly increased the number of nMA-INA6 cells and decreased the number of MA-INA6 cells (Figure 3F). Furthermore, the nMA-INA6 population contained significantly more cells cycling in the G0/G1 phase than the MA-INA6 population, both in synchronously and asynchronously cycling INA-6 (Figure 3G, Appendix A: Figure 3, 4). The number of nMA-INA6 INA-6 cells increased due to a higher cell division frequency. Taken together, we showed that INA-6 detach from aggregates by generating one temporarily detached daughter cell after cell division, a process that potentially contributes to the initiation of dissemination.

### RNAseq of Non-MSC-Adhering and MSC-Adhering Subpopulations

To characterize the subpopulations separated by WPSC, we conducted RNAseq, revealing 1291 differentially expressed genes nMA-INA6 *vs.* CM-INA6, 484 MA-INA6 *vs.* CM-INA6, and 195 MA-INA6 *vs.* nMA-INA6. We validated RNAseq and found that the differential expression of 18 genes correlated with those measured with qPCR for each pairwise comparison (Figure 4C–E, Appendix A: Figure 5): nMA-INA6 *vs.* CM-INA6 [ $\rho(16) = .803$ ,  $p = 6.09 \times 10^{-5}$ ], MA-INA6 *vs.* CM-INA6 [ $\rho(16) = .827$ ,  $p = 2.30 \times 10^{-5}$ ], and MA-INA6 *vs.* nMA-INA6 [ $\rho(16) = .746$ ,  $p = 3.74 \times 10^{-4}$ ] (Spearman’s rank correlation). One of the 18 genes (*MUC1*) measured by qPCR showed a mean expression opposite to that obtained by RNAseq nMA-INA6 *vs.* CM-INA6, although the difference was insignificant (Figure 4C). For nMA-INA6 *vs.* CM-INA6, the difference in expression measured by qPCR was significant for only two of the 11 genes (*DKK1*, *OPG*), whereas the other genes (*DKK1*, *OPG*, *BCL6*, *BMP4*, *BTG2*, *IL10RB*, *IL24*, *NOTCH2*, *TNFRSF1A*, *TRAF5*) only confirmed the tendency measured by RNAseq (Figure 4C–E). For MA-INA6 *vs.* CM-INA6, qPCR validated the significant upregulation of seven genes (*DKK1*, *OPG*, *BCL6*, *BMP4*, *BTG2*, *IL10RB*, *IL24*, *NOTCH2*, *TNFRSF1A*, *TRAF5*, *TGM2*, *DCN*, *LOX*, *MMP14*, *MMP2*, *CXCL12*, *CXCL8*), whereas the downregulation of *BMP4* was insignificant.

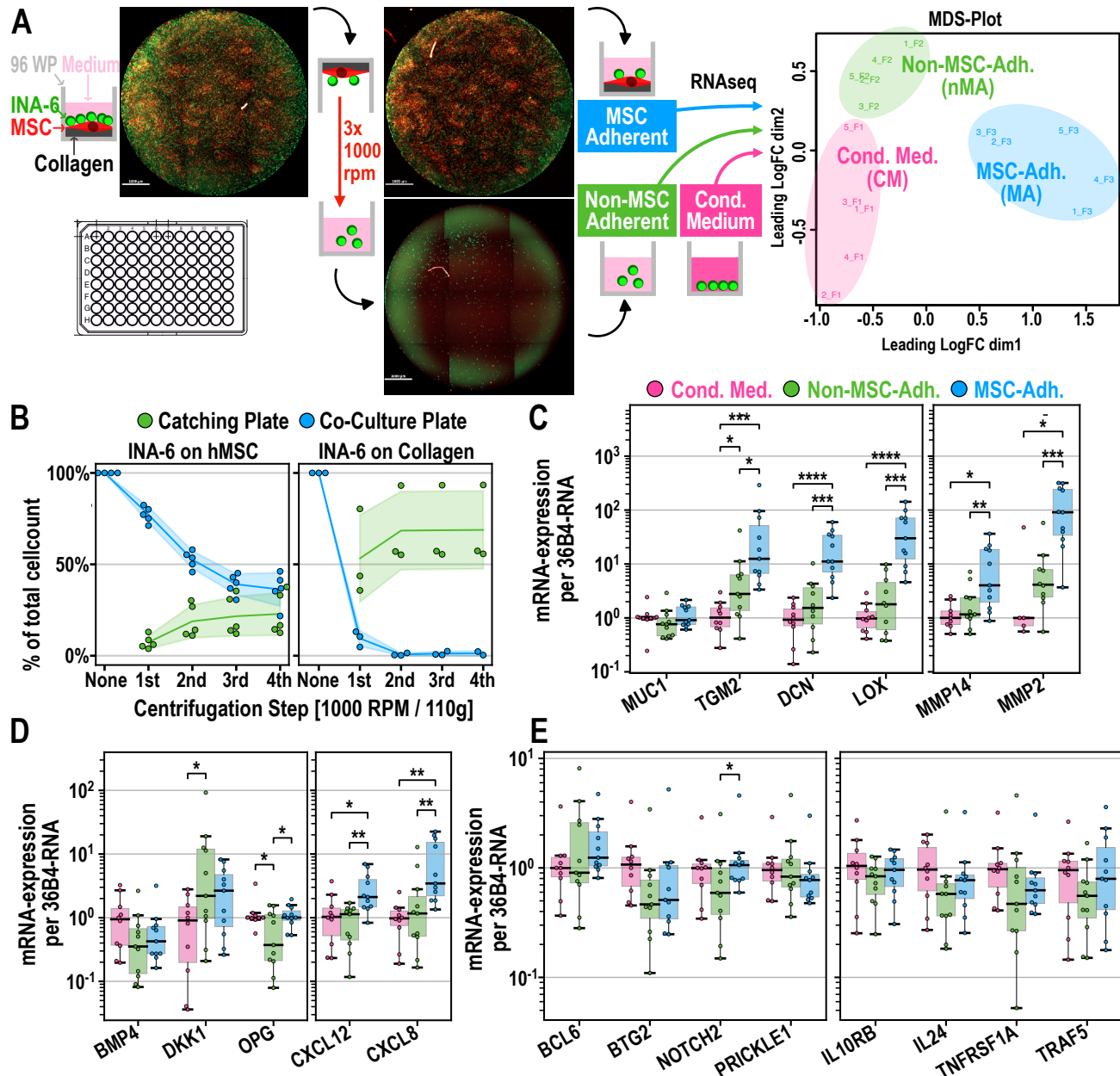


**Figure 4:** Separation and gene expression of INA-6 subpopulations. **A:** Schematic of “Well-Plate Sandwich Centrifugation” (WPSC) separating nMA- from MA-INA6. A co-culture 96-well plate is turned upside down and attached on top of a “catching plate”, forming a “well-plate sandwich”. nMA-INA6 cells are collected in the catching plate by subsequent rounds of centrifugation and gentle washing. MA-INA6 are enzymatically dissociated from hMSCs or by rough pipetting. Subsequent RNAseq of MSC-interacting subpopulations reveals distinct expression clusters [right, multidimensional scaling plot (MDS) ( $n = 5$ )]. **B:** Separation was microscopically tracked after each centrifugation step. **C-E:** RT-qPCR of genes derived from RNAseq results. Expression was normalized to the median of CM-INA6. Samples include those used for RNAseq and six further co-cultures ( $n = 11$ ; non-detects were discarded). **C:** Adhesion factors, ECM proteins, and matrix metalloproteinases. **D:** Factors involved in bone remodeling and bone homing chemokines. **E:** Factors involved in (immune) signaling. **Statistics:** (C-E): Paired t-test. Datapoints represent the mean of three (B-E) technical replicates. INA-6 were isolated from independent co-cultures with hMSCs from five (A, B), nine (C-E) unique donors.

Lorem ipsum dolor sit amet, consetetur sadipscing elitr, sed diam nonumy eirmod tempor  
invidunt ut labore et dolore magna aliquyam erat, sed diam

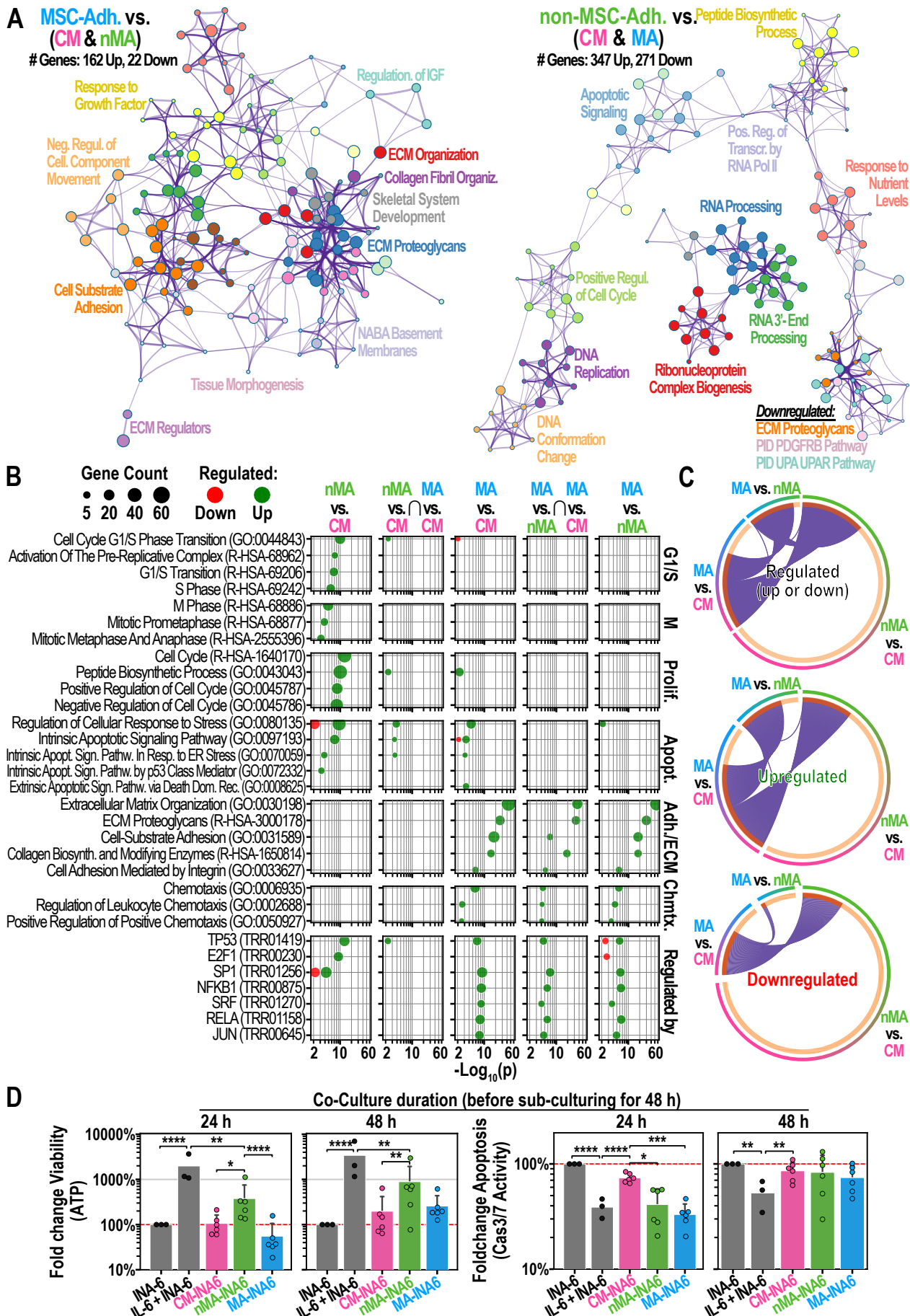


**Figure 5:** Functional analysis of MSC-interacting subpopulations (**A-C**): Functional enrichment analysis of differentially expressed genes (from RNAseq) using Metascape. **A:** Gene ontology (GO) cluster analysis of gene lists that are unique for MA (left) or nMA (right) INA-6. Circle nodes represent subsets of input genes falling into similar GO-term. Node size grows with the number of input genes. Node color defines a shared parent GO-term. Two nodes with a similarity score  $> 0.3$  are linked. **B:** Enrichment analysis of pairwise comparisons between MA subpopulations and their overlaps (arranged in columns). GO terms were manually picked and categorized (arranged in rows). Raw Metascape results are shown in Appendix A: Figure 6. For each GO-term, the p-values (x-axis) and the counts of matching input genes (circle size) were plotted. The lowest row shows enrichment of gene lists from the TRRUST-database. **C:** Circos plots by Metascape. Sections of a circle represent lists of differentially expressed genes. Purple lines connect same genes appearing in two gene lists.  $\cap$ : Overlapping groups, MA: MSC-adhering, nMA: non-MSC-adhering, CM: MSC-Conditioned Medium. **D:** INA-6 were co-cultured on confluent hMSC for 24 h or 48 h, separated by WPSC and sub-cultured for 48 h under IL-6 withdrawal ( $n = 6$ ), except the control (IL-6 + INA-6) ( $n = 3$ ). Signals were normalized (red line) to INA-6 cells grown without hMSCs and IL-6 ( $n = 3$ ). **Statistics:** (D): Paired t-test, two-factor RM-ANOVA. Datapoints represent the mean of four technical replicates. INA-6 were isolated from independent co-cultures with hMSCs from six unique donors.

Lorem ipsum dolor sit amet, consetetur sadipscing elitr, sed diam nonumy eirmod tempor invidunt ut labore et dolore magna aliquyam erat, sed diam Lorem ipsum dolor sit amet, consetetur sadipscing elitr, sed diam nonumy eirmod tempor invidunt ut labore et dolore magna aliquyam erat, sed diam voluptua. At vero eos et accusam et justo duo dolores et ea rebum. Stet Lorem ipsum dolor sit amet, consetetur sadipscing elitr, sed diam nonumy eirmod tempor invidunt ut labore et dolore magna aliquyam erat, sed diam voluptua. At vero eos et accusam et justo duo dolores et ea rebum. Stet

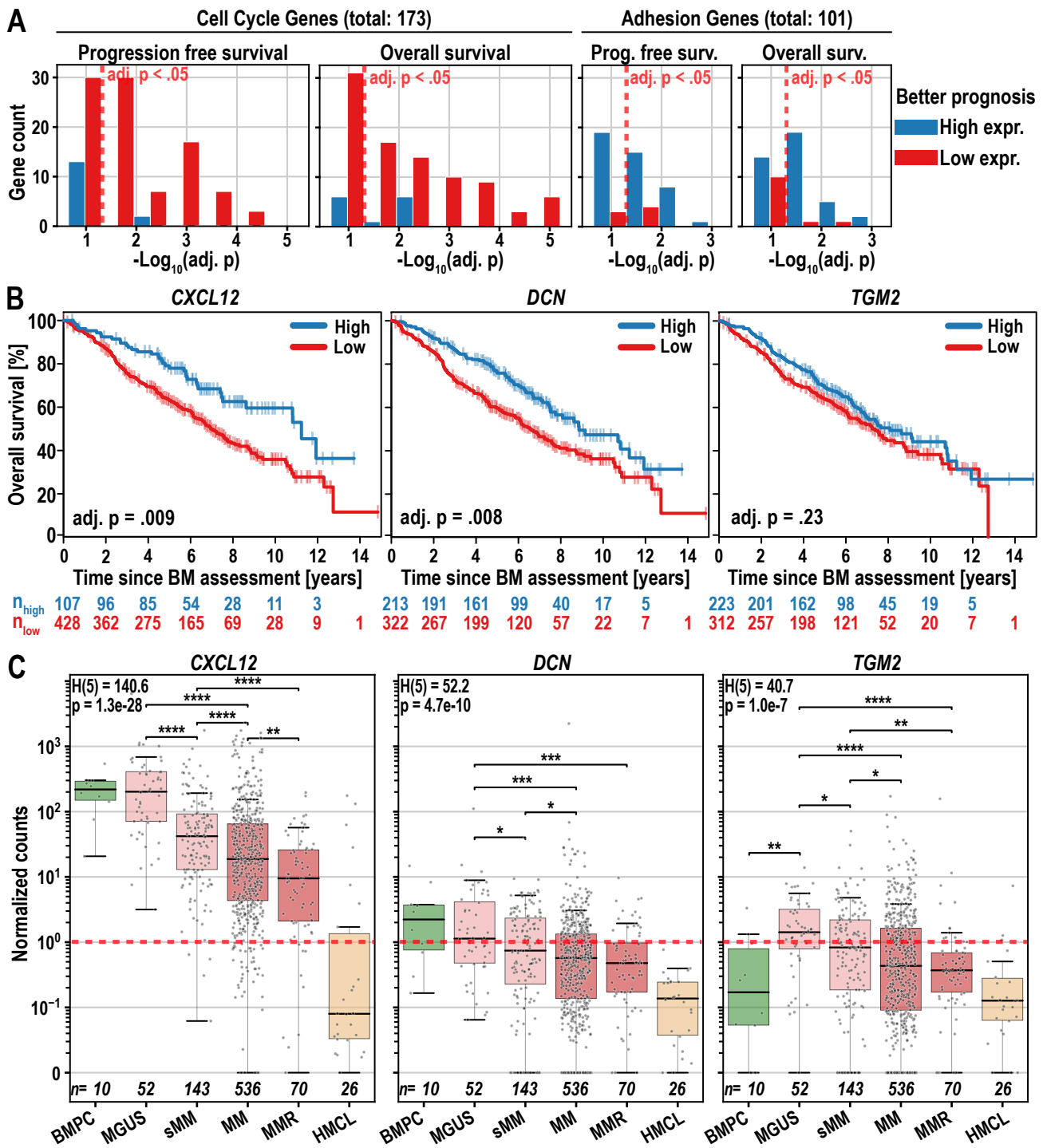


**Figure 6:** Survival of patients with multiple myeloma regarding the expression levels of adhesion and bone retention genes. **A:** p-value distribution of genes associated with patient survival ( $n = 535$ ) depending on high or low expression levels. Red dashed line marks the significance threshold of  $p\text{-adj} = 0.05$ . Histogram of p-values was plotted using a bin width of  $-\log_{10}(0.05)/2$ . Patients with high and low gene expression were delineated using maximally selected rank statistics (maxstat). **B:** Survival curves for three genes taken from the list of adhesion genes shown in (A), maxstat thresholds defining high and low expression were: *CXCL12*: 81.08; *DCN*: 0.75; *TGM2*: 0.66 normalized counts. **C:** Gene expression (RNAseq,  $n = 873$ ) measured in normalized counts (edgeR) of *CXCL12*, *DCN* in Bone Marrow Plasma Cell (BMPC), Monoclonal Gammopathy of Undetermined Significance (MGUS), smoldering Multiple Myeloma (sMM), Multiple Myeloma (MM), Multiple – *Continued on next page*

*Continued from previous page* – Myeloma Relapse (MMR), Human Myeloma Cell Lines (HMCL). The red dashed line marks one normalized read count. **Statistics:** (A, B): Log-rank test; (C): Kruskal-Wallis, Mann–Whitney U Test. All *p*-values were corrected using the Benjamini-Hochberg procedure.

Lore ipsum dolor sit amet, consetetur sadipscing elitr, sed diam nonumy eirmod tempor invidunt ut labore et dolore magna aliquyam erat, sed diam Lorem ipsum dolor sit amet, consetetur sadipscing elitr, sed diam nonumy eirmod tempor invidunt ut labore et dolore magna aliquyam erat, sed diam voluptua. At vero eos et accusam et justo duo dolores et ea rebum. Stet Lorem ipsum dolor sit amet, consetetur sadipscing elitr, sed diam nonumy eirmod tempor invidunt ut labore et dolore magna aliquyam erat, sed diam voluptua. At vero eos et accusam et justo duo dolores et ea rebum. Stet

**Table 1:** Adhesion and ECM genes (shown in Figure 6A) were filtered by their association with patient survival (*p*-adj. < 0.01) and were categorized as continuously downregulated during disease progression. The complete list is presented in Appendix A: Table 2. Bone Marrow Plasma Cells (BMPC), Monoclonal Gammapathy of Undetermined Significance (MGUS), smoldering Multiple Myeloma (sMM), Multiple Myeloma (MM), and Multiple Myeloma Relapse (MMR). *p*-unc: unadjusted *p*-values; *p*-adj: *p*-values adjusted using the Benjamini-Hochberg method with 101 genes.

Regulation during disease progression	Gene	Ensemble ID	Progression Free / Overall Survival	Better Prognosis with high/low expression	Association of expression with survival	
					[ <i>p</i> -unc]	[ <i>p</i> -adj]
Not Downregulated (or overall low expression)	<b>CCNE2</b>	ENSG00000175305	Overall	low	5.34E-04	8.64E-03
	<b>MMP2</b>	ENSG00000087245	Prog. Free	high	2.29E-05	2.32E-03
	<b>OSMR</b>	ENSG00000145623	Prog. Free	high	5.67E-04	7.15E-03
Continuously Downregulated (BMPC > MGUS > sMM > MM > MMR)	<b>AXL</b>	ENSG00000167601	Overall	high	3.64E-05	1.84E-03
	<b>COL1A1</b>	ENSG00000108821	Prog. Free	high	3.03E-04	4.37E-03
			Overall	high	5.93E-04	8.64E-03
	<b>CXCL12</b>	ENSG00000107562	Prog. Free	high	1.16E-04	2.93E-03
			Overall	high	6.48E-04	8.64E-03
	<b>CYP1B1</b>	ENSG00000138061	Overall	high	6.84E-04	8.64E-03
	<b>DCN</b>	ENSG00000011465	Overall	high	2.47E-04	8.33E-03
	<b>LRP1</b>	ENSG00000123384	Overall	high	4.34E-04	8.64E-03
	<b>LTBP2</b>	ENSG00000119681	Prog. Free	high	9.03E-05	2.93E-03
	<b>CYP1B1</b>	ENSG00000138061	Overall	high	6.84E-04	8.64E-03
	<b>DCN</b>	ENSG00000011465	Overall	high	2.47E-04	8.33E-03
	<b>LRP1</b>	ENSG00000123384	Overall	high	4.34E-04	8.64E-03
	<b>LTBP2</b>	ENSG00000119681	Prog. Free	high	9.03E-05	2.93E-03
	<b>MFAP5</b>	ENSG00000197614	Prog. Free	high	2.43E-04	4.09E-03
	<b>MMP14</b>	ENSG00000157227	Prog. Free	high	6.93E-05	2.93E-03

*Continued on next page*

**Table 1 – Continued from previous page**

	MYL9	ENSG00000101335	Prog. Free	high	1.46E-04	2.95E-03
			Overall	high	1.56E-05	1.57E-03

Lorem ipsum dolor sit amet, consetetur sadipscing elitr, sed diam nonumy eirmod tempor invidunt ut labore et dolore magna aliquyam erat, sed diam voluptua. At vero eos et accusam et justo duo dolores et ea rebum. Stet Lorem ipsum dolor sit amet, consetetur sadipscing elitr, sed diam nonumy eirmod tempor invidunt ut labore et dolore magna aliquyam erat, sed diam voluptua. At vero eos et accusam et justo duo dolores et ea rebum. Stet

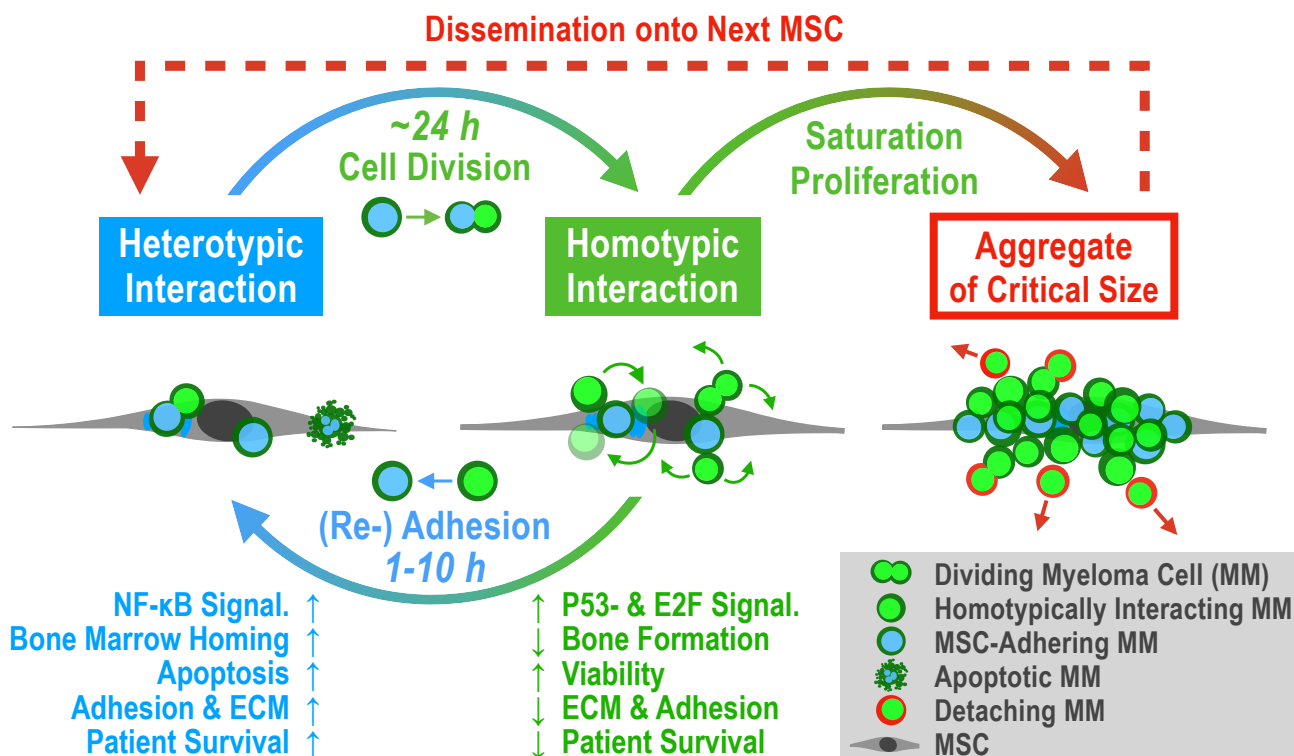


**Figure 7:** Proposed model of “Detached Daughter Driven Dissemination” (DDDD) in aggregating multiple myeloma. **Heterotypic Interaction:** Malignant plasma cells colonize the bone marrow microenvironment by adhering to an MSC (or osteoblast, ECM, etc.) to maximize growth and survival through paracrine and adhesion mediated signaling, even if contact may trigger initial apoptosis. Gene expression will focus on establishing a strong anchor within the bone marrow, but also on attracting other myeloma cells (via secretion of ECM factors and CXCL12/CXCL8, respectively). **Cell Division:** Cell fission can generate one daughter cell that no longer adheres to the MSC (nMA). **Homotypic Interaction:** If myeloma cells have the capacity to grow as aggregates, the daughter cell stays attached to their MSC-adhering mother cell (MA). **Re-Adhesion:** The daughter cell “rolls around” the mother cell until it re-adheres to the MSC. Our model estimates the rolling duration to be 1–10 h long. **Proliferation & Saturation:** We estimate that a single myeloma cell covers one MSC completely after roughly four population doublings. When heterotypic adhesion is saturated, subsequent daughter cells benefit from a homotypic interaction, since they stay close to growth-factor secreting MSCs and focus gene expression on proliferation (e.g. driven by E2F) and not adhesion (driven by NF- B). **Critical Size:** Homotypic interaction is weaker than heterotypic interaction, and each cell fission destabilizes the aggregate. Hence, detachment of myeloma cells may depend mostly on aggregate size. **Dissemination:** After myeloma cells have detached, they gained a viability advantage through IL-6-independence (with unknown duration), which enhances their survival outside of the bone marrow and allows them to spread throughout the body.

Lorem ipsum dolor sit amet, consetetur sadipscing elitr, sed diam nonumy eirmod tempor invidunt ut labore et dolore magna aliquyam erat, sed diam voluptua. At vero eos et accusam et justo duo dolores et ea rebum. Stet Lorem ipsum dolor sit amet, consetetur sadipscing elitr, sed diam nonumy eirmod tempor invidunt ut labore et dolore magna aliquyam erat, sed diam voluptua. At vero eos et accusam et justo duo dolores et ea rebum. Stet

## Discussion

lorem ipsum

## References

- Abadi, M., Agarwal, A., Barham, P., Brevdo, E., Chen, Z., Citro, C., ... Zheng, X. (2016, March). *TensorFlow: Large-Scale Machine Learning on Heterogeneous Distributed Systems* (No. arXiv:1603.04467). arXiv. Retrieved 2024-03-07, from <http://arxiv.org/abs/1603.04467> doi: 10.48550/arXiv.1603.04467
- Aggarwal, R., Ghobrial, I. M., & Roodman, G. D. (2006, October). Chemokines in multiple myeloma. *Experimental hematology*, 34(10), 1289–1295. Retrieved 2023-04-02, from <https://www.ncbi.nlm.nih.gov/pmc/articles/PMC3134145/> doi: 10.1016/j.exphem.2006.06.017
- Akhmetzyanova, I., McCarron, M. J., Parekh, S., Chesi, M., Bergsagel, P. L., & Fooksman, D. R. (2020). Dynamic CD138 surface expression regulates switch between myeloma growth and dissemination. *Leukemia*, 34(1), 245–256. Retrieved 2023-04-04, from <https://www.ncbi.nlm.nih.gov/pmc/articles/PMC6923614/> doi: 10.1038/s41375-019-0519-4
- Alcorta-Sevillano, N., Macías, I., Infante, A., & Rodríguez, C. I. (2020, December). Deciphering the Relevance of Bone ECM Signaling. *Cells*, 9(12), 2630. Retrieved 2023-12-20, from <https://www.ncbi.nlm.nih.gov/pmc/articles/PMC7762413/> doi: 10.3390/cells9122630
- Alsayed, Y., Ngo, H., Runnels, J., Leleu, X., Singha, U. K., Pitsillides, C. M., ... Ghobrial, I. M. (2007, April). Mechanisms of regulation of CXCR4/SDF-1 (CXCL12)-dependent migration and homing in multiple myeloma. *Blood*, 109(7), 2708–2717. doi: 10.1182/blood-2006-07-035857
- Anders, S., Pyl, P. T., & Huber, W. (2015, January). HTSeq—a Python framework to work with high-throughput sequencing data. *Bioinformatics (Oxford, England)*, 31(2), 166–169. doi: 10.1093/bioinformatics/btu638
- Andrews, S. (2010). *FASTQC. A quality control tool for high throughput sequence data*.
- Armstrong, R. A. (2014, September). When to use the Bonferroni correction. *Ophthalmic & Physiological Optics: The Journal of the British College of Ophthalmic Opticians (Optometrists)*, 34(5), 502–508. doi: 10.1111/opo.12131
- Barzilay, R., Ben-Zur, T., Bulvik, S., Melamed, E., & Offen, D. (2009, May). Lentiviral delivery of LMX1a enhances dopaminergic phenotype in differentiated human bone marrow mesenchymal stem cells. *Stem cells and development*, 18(4), 591–601. doi: 10.1089/scd.2008.0138
- Begley, C. G., & Ioannidis, J. P. A. (2015, January). Reproducibility in science: Improving the standard for basic and preclinical research. *Circulation Research*, 116(1), 116–126. doi: 10.1161/CIRCRESAHA.114.303819
- Bianco, P. (2014). "Mesenchymal" stem cells. *Annual review of cell and developmental biology*, 30, 677–704. doi: 10.1146/annurev-cellbio-100913-013132
- Bladé, J., Beksac, M., Caers, J., Jurczyszyn, A., von Lilienfeld-Toal, M., Moreau, P., ... Richardson, P. (2022, March). Extramedullary disease in multiple myeloma: A systematic literature review. *Blood Cancer Journal*, 12(3), 1–10. Retrieved 2023-03-24, from <https://www.nature.com/articles/s41408-022-00643-3> doi: 10.1038/s41408-022-00643-3
- Bondi, A. B. (2000, September). Characteristics of scalability and their impact on performance. In *Proceedings of the 2nd international workshop on Software and performance* (pp. 195–203). New York, NY, USA: Association for Computing Machinery. Retrieved 2024-03-07, from <https://dl.acm.org/doi/10.1145/350391.350432> doi: 10.1145/350391.350432
- Boswell, D., & Foucher, T. (2011). *The Art of Readable Code: Simple and Practical Techniques for Writing Better Code*. "O'Reilly Media, Inc."
- Brooke, J. (1996, January). SUS – a quick and dirty usability scale. In (pp. 189–194).
- Burger, R., Guenther, A., Bakker, F., Schmalzing, M., Bernand, S., Baum, W., ... Gramatzki, M. (2001). Gp130 and ras mediated signaling in human plasma cell line INA-6: A cytokine-regulated tumor model for plasmacytoma. *The Hematology Journal: The Official Journal of the European Haematology Association*, 2(1), 42–53. doi: 10.1038/sj.thj.6200075

- Burger, R., Günther, A., Bakker, F., Schmalzing, M., Bernand, S., Baum, W., ... Gramatzki, M. (2001, January). Gp130 and ras mediated signaling in human plasma cell line INA6: A cytokine-regulated tumor model for plasmacytoma. *Hematology Journal - HEMATOL J*, 2, 42–53. doi: 10.1038/sj.thj.6200075
- Bustin, S. A. (2014, December). The reproducibility of biomedical research: Sleepers awake! *Biomolecular Detection and Quantification*, 2, 35–42. Retrieved 2024-03-18, from <https://www.sciencedirect.com/science/article/pii/S2214753515000030> doi: 10.1016/j.bdq.2015.01.002
- Caplan, A. (1991). Mesenchymal stem cells. *Journal of orthopaedic research : official publication of the Orthopaedic Research Society*, 9(5), 641–50. Retrieved from <http://www.ncbi.nlm.nih.gov/pubmed/1870029> doi: 10.1002/jor.1100090504
- Caplan, A. I. (1994, July). The mesengenic process. *Clinics in plastic surgery*, 21(3), 429–435.
- Carlson, M. (2016). Org.Hs.eg.db. *Bioconductor*. Retrieved 2023-06-09, from <http://bioconductor.org/packages/org.Hs.eg.db/> doi: 10.18129/B9.bioc.org.Hs.eg.db
- Chacon, S., & Straub, B. (2024, March). *Git - Book*. Retrieved 2024-03-07, from <https://git-scm.com/book/de/v2>
- Charlier, F., Weber, M., Izak, D., Harkin, E., Magnus, M., Lalli, J., ... Repplinger, S. (2022, October). *Trevismd/statannotations: V0.5*. Zenodo. Retrieved 2023-11-16, from <https://zenodo.org/record/7213391> doi: 10.5281/ZENODO.7213391
- Chatterjee, M., Hönenmann, D., Lentzsch, S., Bommert, K., Sers, C., Herrmann, P., ... Bargou, R. C. (2002, November). In the presence of bone marrow stromal cells human multiple myeloma cells become independent of the IL-6/gp130/STAT3 pathway. *Blood*, 100(9), 3311–3318. doi: 10.1182/blood-2002-01-0102
- Cooper, G. M. (2000). The Cell: A Molecular Approach. 2nd Edition. *Sinauer Associates*, Proliferation in Development and Differentiation. Retrieved from <https://www.ncbi.nlm.nih.gov/books/NBK9906/>
- da Silva Meirelles, L., Chagastelles, P. C., & Nardi, N. B. (2006, June). Mesenchymal stem cells reside in virtually all post-natal organs and tissues. *Journal of cell science*, 119(Pt 11), 2204–2213. doi: 10.1242/jcs.02932
- Dobin, A., Davis, C. A., Schlesinger, F., Drenkow, J., Zaleski, C., Jha, S., ... Gingeras, T. R. (2013, January). STAR: Ultrafast universal RNA-seq aligner. *Bioinformatics*, 29(1), 15–21. Retrieved 2023-05-27, from <https://www.ncbi.nlm.nih.gov/pmc/articles/PMC3530905/> doi: 10.1093/bioinformatics/bts635
- Dominici, M., Le Blanc, K., Mueller, I., Slaper-Cortenbach, I., Marini, F., Krause, D., ... Horwitz, E. (2006). Minimal criteria for defining multipotent mesenchymal stromal cells. The International Society for Cellular Therapy position statement. *Cytotherapy*, 8(4), 315–317. doi: 10.1080/14653240600855905
- Duvall, P., Matyas, S., & Glover, A. (2007). *Continuous integration: Improving software quality and reducing risk*. Pearson Education. Retrieved from <https://books.google.de/books?id=PV9qfEdv9L0C>
- Dziadowicz, S. A., Wang, L., Akhter, H., Aesoph, D., Sharma, T., Adjeroth, D. A., ... Hu, G. (2022, January). Bone Marrow Stroma-Induced Transcriptome and Regulome Signatures of Multiple Myeloma. *Cancers*, 14(4), 927. Retrieved 2022-10-25, from <https://www.mdpi.com/2072-6694/14/4/927> doi: 10.3390/cancers14040927
- Ekmekci, B., McAnany, C. E., & Mura, C. (2016, July). An Introduction to Programming for Biologists: A Python-Based Primer. *PLOS Computational Biology*, 12(6), e1004867. Retrieved 2024-03-10, from <https://journals.plos.org/ploscompbiol/article?id=10.1371/journal.pcbi.1004867> doi: 10.1371/journal.pcbi.1004867
- Ewels, P., Magnusson, M., Lundin, S., & Käller, M. (2016, October). MultiQC: Summarize analysis results for multiple tools and samples in a single report. *Bioinformatics*, 32(19), 3047–3048. Retrieved 2023-06-09, from <https://doi.org/10.1093/bioinformatics/btw354> doi: 10.1093/bioinformatics/btw354
- Fazeli, P. K., Horowitz, M. C., MacDougald, O. A., Scheller, E. L., Rodeheffer, M. S., Rosen, C. J., & Klibanski, A. (2013, March). Marrow Fat and Bone—New Perspectives. *The Journal of Clinical Endocrinology and Metabolism*, 98(3), 935–945. Retrieved 2023-12-20, from <https://www.ncbi.nlm.nih.gov/pmc/articles/>

- PMC3590487/ doi: 10.1210/jc.2012-3634
- Fernandez-Rebollo, E., Mentrup, B., Ebert, R., Franzen, J., Abagnale, G., Sieben, T., ... Wagner, W. (2017, July). Human Platelet Lysate versus Fetal Calf Serum: These Supplements Do Not Select for Different Mesenchymal Stromal Cells. *Scientific Reports*, 7, 5132. Retrieved 2023-05-02, from <https://www.ncbi.nlm.nih.gov/pmc/articles/PMC5506010/> doi: 10.1038/s41598-017-05207-1
- Frassanito, M. A., Cusmai, A., Iodice, G., & Dammacco, F. (2001, January). Autocrine interleukin-6 production and highly malignant multiple myeloma: Relation with resistance to drug-induced apoptosis. *Blood*, 97(2), 483–489. doi: 10.1182/blood.v97.2.483
- Friedenstein, A., & Kuralesova, A. I. (1971, August). Osteogenic precursor cells of bone marrow in radiation chimeras. *Transplantation*, 12(2), 99–108.
- Friedenstein, A. J., Piatetzky-Shapiro, I. I., & Petrakova, K. V. (1966, December). Osteogenesis in transplants of bone marrow cells. *Journal of embryology and experimental morphology*, 16(3), 381–390.
- Gabr, M. M., Zakaria, M. M., Refaie, A. F., Ismail, A. M., Abou-El-Mahasen, M. A., Ashamallah, S. A., ... Ghoneim, M. A. (2013). Insulin-producing cells from adult human bone marrow mesenchymal stem cells control streptozotocin-induced diabetes in nude mice. *Cell transplantation*, 22(1), 133–145. doi: 10.3727/096368912X647162
- García-Ortiz, A., Rodríguez-García, Y., Encinas, J., Maroto-Martín, E., Castellano, E., Teixidó, J., & Martínez-López, J. (2021, January). The Role of Tumor Microenvironment in Multiple Myeloma Development and Progression. *Cancers*, 13(2). Retrieved 2021-02-02, from <https://www.ncbi.nlm.nih.gov/pmc/articles/PMC7827690/> doi: 10.3390/cancers13020217
- Gentleman. (n.d.). *Bioconductor - BiocViews*. Retrieved 2023-06-09, from <https://bioconductor.org/packages/3.17/BiocViews.html>
- Ghobrial, I. M. (2012, July). Myeloma as a model for the process of metastasis: Implications for therapy. *Blood*, 120(1), 20–30. Retrieved 2022-10-15, from <https://www.ncbi.nlm.nih.gov/pmc/articles/PMC3390959/> doi: 10.1182/blood-2012-01-379024
- Glavey, S. V., Naba, A., Manier, S., Clauser, K., Tahri, S., Park, J., ... Ghobrial, I. M. (2017, November). Proteomic characterization of human multiple myeloma bone marrow extracellular matrix. *Leukemia*, 31(11), 2426–2434. Retrieved 2023-09-05, from <https://www.nature.com/articles/leu2017102> doi: 10.1038/leu.2017.102
- Gomez-Cabrero, D., Abugessaisa, I., Maier, D., Teschendorff, A., Merkenschlager, M., Gisel, A., ... Tegnér, J. (2014, March). Data integration in the era of omics: Current and future challenges. *BMC Systems Biology*, 8(2), I1. Retrieved 2024-03-18, from <https://doi.org/10.1186/1752-0509-8-S2-I1> doi: 10.1186/1752-0509-8-S2-I1
- Gómez-López, G., Dopazo, J., Cigudosa, J. C., Valencia, A., & Al-Shahrour, F. (2019, May). Precision medicine needs pioneering clinical bioinformaticians. *Briefings in Bioinformatics*, 20(3), 752–766. doi: 10.1093/bib/bbx144
- Goodman, S. N., Fanelli, D., & Ioannidis, J. P. A. (2016, June). What does research reproducibility mean? *Science Translational Medicine*, 8(341), 341ps12–341ps12. Retrieved 2024-03-18, from <https://www.science.org/doi/10.1126/scitranslmed.aaf5027> doi: 10.1126/scitranslmed.aaf5027
- Gosselin, R.-D. (2021, February). Insufficient transparency of statistical reporting in preclinical research: A scoping review. *Scientific Reports*, 11(1), 3335. Retrieved 2024-03-11, from <https://www.nature.com/articles/s41598-021-83006-5> doi: 10.1038/s41598-021-83006-5
- Gramatzki, M., Burger, R., Trautman, U., Marschalek, R., Lorenz, H., Hansen-Hagge, T., ... Kalden, J. (1994). Two new interleukin-6 dependent plasma cell lines carrying a chromosomal abnormality involving the IL-6 gene locus. , 84 Suppl. 1, 173a-173a. Retrieved 2023-03-24, from <https://www.cellosaurus.org/cellopublishing/>

- CLPUB00060
- Greenstein, S., Krett, N. L., Kurosawa, Y., Ma, C., Chauhan, D., Hideshima, T., ... Rosen, S. T. (2003, April). Characterization of the MM.1 human multiple myeloma (MM) cell lines: A model system to elucidate the characteristics, behavior, and signaling of steroid-sensitive and -resistant MM cells. *Experimental Hematology*, 31(4), 271–282. doi: 10.1016/s0301-472x(03)00023-7
- Gronthos, S., Graves, S. E., Ohta, S., & Simmons, P. J. (1994, December). The STRO-1+ fraction of adult human bone marrow contains the osteogenic precursors. *Blood*, 84(12), 4164–4173.
- Harrington, D. P., & Fleming, T. R. (1982). A Class of Rank Test Procedures for Censored Survival Data. *Biometrika*, 69(3), 553–566. Retrieved 2023-08-07, from <https://www.jstor.org/stable/2335991> doi: 10.2307/2335991
- Harris, C. R., Millman, K. J., van der Walt, S. J., Gommers, R., Virtanen, P., Cournapeau, D., ... Oliphant, T. E. (2020, September). Array programming with NumPy. *Nature*, 585(7825), 357–362. Retrieved 2023-08-09, from <https://www.nature.com/articles/s41586-020-2649-2> doi: 10.1038/s41586-020-2649-2
- Hideshima, T., Mitsiades, C., Tonon, G., Richardson, P. G., & Anderson, K. C. (2007, August). Understanding multiple myeloma pathogenesis in the bone marrow to identify new therapeutic targets. *Nature Reviews Cancer*, 7(8), 585–598. Retrieved 2023-02-07, from <https://www.nature.com/articles/nrc2189> doi: 10.1038/nrc2189
- Hothorn, T., & Lausen, B. (n.d.). *Maximally Selected Rank Statistics in R*. Retrieved from <http://cran.r-project.org/web/packages/maxstat/index.html>.
- Hu, X., Villodre, E. S., Larson, R., Rahal, O. M., Wang, X., Gong, Y., ... Debeb, B. G. (2021, January). Decorin-mediated suppression of tumorigenesis, invasion, and metastasis in inflammatory breast cancer. *Communications Biology*, 4(1), 72. doi: 10.1038/s42003-020-01590-0
- Huang, S.-Y., Lin, H.-H., Yao, M., Tang, J.-L., Wu, S.-J., Hou, H.-A., ... Tien, H.-F. (2015). Higher Decorin Levels in Bone Marrow Plasma Are Associated with Superior Treatment Response to Novel Agent-Based Induction in Patients with Newly Diagnosed Myeloma - A Retrospective Study. *PLoS One*, 10(9), e0137552. doi: 10.1371/journal.pone.0137552
- Hunter, J. D. (2007, May). Matplotlib: A 2D Graphics Environment. *Computing in Science & Engineering*, 9(3), 90–95. Retrieved 2023-11-15, from <https://ieeexplore.ieee.org/document/4160265> doi: 10.1109/MCSE.2007.55
- Incerti, D., Thom, H., Baio, G., & Jansen, J. P. (2019, May). R You Still Using Excel? The Advantages of Modern Software Tools for Health Technology Assessment. *Value in Health*, 22(5), 575–579. Retrieved 2024-03-11, from <https://www.sciencedirect.com/science/article/pii/S1098301519300506> doi: 10.1016/j.jval.2019.01.003
- Jansen, B. J. H., Gilissen, C., Roelofs, H., Schaap-Oziemlak, A., Veltman, J. A., Raymakers, R. A. P., ... Adema, G. J. (2010, April). Functional differences between mesenchymal stem cell populations are reflected by their transcriptome. *Stem cells and development*, 19(4), 481–490. doi: 10.1089/scd.2009.0288
- Kaplan, E. L., & Meier, P. (1958, June). Nonparametric Estimation from Incomplete Observations. *Journal of the American Statistical Association*, 53(282), 457–481. Retrieved 2023-08-07, from <http://www.tandfonline.com/doi/abs/10.1080/01621459.1958.10501452> doi: 10.1080/01621459.1958.10501452
- Katz, B.-Z. (2010, June). Adhesion molecules—The lifelines of multiple myeloma cells. *Seminars in Cancer Biology*, 20(3), 186–195. Retrieved 2021-07-04, from <https://linkinghub.elsevier.com/retrieve/pii/S1044579X10000246> doi: 10.1016/j.semcan.2010.04.003
- Kawano, M. M., Huang, N., Tanaka, H., Ishikawa, H., Sakai, A., Tanabe, O., ... Kuramoto, A. (1991, December). Homotypic cell aggregations of human myeloma cells with ICAM-1 and LFA-1 molecules. *British Journal of Haematology*, 79(4), 583–588. doi: 10.1111/j.1365-2141.1991.tb08085.x

- Kazman, R., Bianco, P., Ivers, J., & Klein, J. (2020, December). *Maintainability* (Report). Carnegie Mellon University. Retrieved 2024-03-07, from <https://kilthub.cmu.edu/articles/report/Maintainability/12954908/1> doi: 10.1184/R1/12954908.v1
- Kibler, C., Schermutzki, F., Waller, H. D., Timpl, R., Müller, C. A., & Klein, G. (1998, June). Adhesive interactions of human multiple myeloma cell lines with different extracellular matrix molecules. *Cell Adhesion and Communication*, 5(4), 307–323. doi: 10.3109/15419069809040300
- Krekel, H., Oliveira, B., Pfannschmidt, R., Bruynooghe, F., Laugher, B., & Bruhin, F. (2004). *Pytest*. Retrieved from <https://github.com/pytest-dev/pytest>
- Kuric, M., & Ebert, R. (2024, March). Plotastic: Bridging Plotting and Statistics in Python. *Journal of Open Source Software*, 9(95), 6304. Retrieved 2024-03-11, from <https://joss.theoj.org/papers/10.21105/joss.06304> doi: 10.21105/joss.06304
- Lai, T.-Y., Cao, J., Ou-Yang, P., Tsai, C.-Y., Lin, C.-W., Chen, C.-C., ... Lee, C.-Y. (2022, April). Different methods of detaching adherent cells and their effects on the cell surface expression of Fas receptor and Fas ligand. *Scientific Reports*, 12(1), 5713. Retrieved 2023-06-01, from <https://www.nature.com/articles/s41598-022-09605-y> doi: 10.1038/s41598-022-09605-y
- Li, H., Handsaker, B., Wysoker, A., Fennell, T., Ruan, J., Homer, N., ... 1000 Genome Project Data Processing Subgroup (2009, August). The Sequence Alignment/Map format and SAMtools. *Bioinformatics*, 25(16), 2078–2079. Retrieved 2023-06-09, from <https://doi.org/10.1093/bioinformatics/btp352> doi: 10.1093/bioinformatics/btp352
- McKinney, W. (2010, January). Data Structures for Statistical Computing in Python. In (pp. 56–61). doi: 10.25080/Majora-92bf1922-00a
- Moreno-Indias, I., Lahti, L., Nedyalkova, M., Elbere, I., Roshchupkin, G., Adilovic, M., ... Zomer, A. L. (2021, February). Statistical and Machine Learning Techniques in Human Microbiome Studies: Contemporary Challenges and Solutions. *Frontiers in Microbiology*, 12. Retrieved 2024-03-18, from <https://www.frontiersin.org/journals/microbiology/articles/10.3389/fmicb.2021.635781/full> doi: 10.3389/fmicb.2021.635781
- Muruganandan, S., Roman, A. A., & Sinal, C. J. (2009, January). Adipocyte differentiation of bone marrow-derived mesenchymal stem cells: Cross talk with the osteoblastogenic program. *Cellular and molecular life sciences : CMLS*, 66(2), 236–253. doi: 10.1007/s00018-008-8429-z
- Myers, G. J., Sandler, C., & Badgett, T. (2011). *The art of software testing* (3rd ed.). Wiley Publishing. Retrieved from <https://malenezi.github.io/malenezi/SE401/Books/114-the-art-of-software-testing-3-edition.pdf>
- Narzt, W., Pichler, J., Pirklbauer, K., & Zwinz, M. (1998, January). A Reusability Concept for Process Automation Software..
- Newville, M., Stensitzki, T., Allen, D. B., & Ingargiola, A. (2014, September). *LMFIT: Non-Linear Least-Square Minimization and Curve-Fitting for Python*. Zenodo. Retrieved 2023-05-30, from <https://zenodo.org/record/11813> doi: 10.5281/zenodo.11813
- Nilsson, K., Bennich, H., Johansson, S. G., & Pontén, J. (1970, October). Established immunoglobulin producing myeloma (IgE) and lymphoblastoid (IgG) cell lines from an IgE myeloma patient. *Clinical and Experimental Immunology*, 7(4), 477–489.
- Nowotschin, S., & Hadjantonakis, A.-K. (2010, August). Cellular dynamics in the early mouse embryo: From axis formation to gastrulation. *Current opinion in genetics & development*, 20(4), 420–427. doi: 10.1016/j.gde.2010.05.008
- Okuno, Y., Takahashi, T., Suzuki, A., Ichiba, S., Nakamura, K., Okada, T., ... Imura, H. (1991, February). In vitro growth pattern of myeloma cells in liquid suspension or semi-solid culture containing interleukin-6.

- International Journal of Hematology*, 54(1), 41–47.
- Paszke, A., Gross, S., Massa, F., Lerer, A., Bradbury, J., Chanan, G., ... Chintala, S. (2019, December). *PyTorch: An Imperative Style, High-Performance Deep Learning Library* (No. arXiv:1912.01703). arXiv. Retrieved 2024-03-07, from <http://arxiv.org/abs/1912.01703> doi: 10.48550/arXiv.1912.01703
- Peng, R. D. (2011, December). Reproducible Research in Computational Science. *Science*, 334(6060), 1226–1227. Retrieved 2024-03-18, from <https://www.science.org/doi/10.1126/science.1213847> doi: 10.1126/science.1213847
- Perneger, T. V. (1998, April). What's wrong with Bonferroni adjustments. *BMJ : British Medical Journal*, 316(7139), 1236–1238. Retrieved 2021-11-24, from <https://www.ncbi.nlm.nih.gov/pmc/articles/PMC1112991/>
- Pittenger, M. F., Mackay, A. M., Beck, S. C., Jaiswal, R. K., Douglas, R., Mosca, J. D., ... Marshak, D. R. (1999). Multilineage Potential of Adult Human Mesenchymal Stem Cells. , 284(April), 143–148. doi: 10.1126/science.284.5411.143
- The Python Language Reference*. (n.d.). Retrieved 2024-03-07, from <https://docs.python.org/3/reference/index.html>
- R Core Team. (2018). *R: A language and environment for statistical computing* [Manual]. Vienna, Austria. Retrieved from <https://www.R-project.org/>
- Radford, A., Wu, J., Child, R., Luan, D., Amodei, D., & Sutskever, I. (2019). Language Models are Unsupervised Multitask Learners.. Retrieved 2024-03-07, from <https://www.semanticscholar.org/paper/Language-Models-are-Unsupervised-Multitask-Learners-Radford-Wu/9405cc0d6169988371b2755e573cc28650d14dfe>
- Rajkumar, S. V., Dimopoulos, M. A., Palumbo, A., Blade, J., Merlini, G., Mateos, M.-V., ... Miguel, J. F. S. (2014, November). International Myeloma Working Group updated criteria for the diagnosis of multiple myeloma. *The Lancet. Oncology*, 15(12), e538–548. doi: 10.1016/S1470-2045(14)70442-5
- Rajkumar, S. V., & Kumar, S. (2020, September). Multiple myeloma current treatment algorithms. *Blood Cancer Journal*, 10(9), 94. Retrieved 2023-07-03, from <https://www.ncbi.nlm.nih.gov/pmc/articles/PMC7523011/> doi: 10.1038/s41408-020-00359-2
- Ramakers, C., Ruijter, J. M., Deprez, R. H., & Moorman, A. F. (2003, March). Assumption-free analysis of quantitative real-time polymerase chain reaction (PCR) data. *Neuroscience Letters*, 339(1), 62–66. Retrieved 2022-11-27, from <https://linkinghub.elsevier.com/retrieve/pii/S0304394002014234> doi: 10.1016/S0304-3940(02)01423-4
- Rayhan, A., & Gross, D. (2023). *The Rise of Python: A Survey of Recent Research*. doi: 10.13140/RG.2.2.27388.92809
- Robinson, M. D., McCarthy, D. J., & Smyth, G. K. (2010, January). edgeR: A Bioconductor package for differential expression analysis of digital gene expression data. *Bioinformatics (Oxford, England)*, 26(1), 139–140. Retrieved from <https://www.ncbi.nlm.nih.gov/pubmed/19910308> doi: 10.1093/bioinformatics/btp616
- Sacchetti, B., Funari, A., Remoli, C., Giannicola, G., Kogler, G., Liedtke, S., ... Bianco, P. (2016). No identical "mesenchymal stem cells" at different times and sites: Human committed progenitors of distinct origin and differentiation potential are incorporated as adventitial cells in microvessels. *Stem Cell Reports*, 6(6), 897–913. Retrieved from <http://dx.doi.org/10.1016/j.stemcr.2016.05.011> doi: 10.1016/j.stemcr.2016.05.011
- Sandve, G. K., Nekrutenko, A., Taylor, J., & Hovig, E. (2013, October). Ten Simple Rules for Reproducible Computational Research. *PLoS Computational Biology*, 9(10), e1003285. Retrieved 2024-03-07, from <https://www.ncbi.nlm.nih.gov/pmc/articles/PMC3812051/> doi: 10.1371/journal.pcbi.1003285
- Sanz-Rodríguez, F., Ruiz-Velasco, N., Pascual-Salcedo, D., & Teixidó, J. (1999, December). Characterization of VLA-4-dependent myeloma cell adhesion to fibronectin and VCAM-1: VLA-4-dependent Myeloma Cell Adhesion. *British Journal of Haematology*, 107(4), 825–834. Retrieved 2023-04-02, from <http://doi.wiley>

- .com/10.1046/j.1365-2141.1999.01762.x doi: 10.1046/j.1365-2141.1999.01762.x
- Seabold, S., & Perktold, J. (2010). Statsmodels: Econometric and Statistical Modeling with Python. In *Python in Science Conference* (pp. 92–96). Austin, Texas. Retrieved 2023-05-29, from <https://conference.scipy.org/proceedings/scipy2010/seabold.html> doi: 10.25080/Majora-92bf1922-011
- Seckinger, A., Delgado, J. A., Moser, S., Moreno, L., Neuber, B., Grab, A., ... Vu, M. D. (2017, March). Target Expression, Generation, Preclinical Activity, and Pharmacokinetics of the BCMA-T Cell Bispecific Antibody EM801 for Multiple Myeloma Treatment. *Cancer Cell*, 31(3), 396–410. Retrieved 2023-07-21, from [https://www.cell.com/cancer-cell/abstract/S1535-6108\(17\)30016-8](https://www.cell.com/cancer-cell/abstract/S1535-6108(17)30016-8) doi: 10.1016/j.ccr.2017.02.002
- Seckinger, A., Hillengass, J., Emde, M., Beck, S., Kimmich, C., Dittrich, T., ... Hose, D. (2018). CD38 as Immunotherapeutic Target in Light Chain Amyloidosis and Multiple Myeloma-Association With Molecular Entities, Risk, Survival, and Mechanisms of Upfront Resistance. *Frontiers in Immunology*, 9, 1676. doi: 10.3389/fimmu.2018.01676
- Shenghui, H., Nakada, D., & Morrison, S. J. (2009). Mechanisms of Stem Cell Self-Renewal. *Annual Review of Cell and Developmental Biology*, 25(1), 377–406. Retrieved from <https://doi.org/10.1146/annurev.cellbio.042308.113248> doi: 10.1146/annurev.cellbio.042308.113248
- Smith, A. M., Niemeyer, K. E., Katz, D. S., Barba, L. A., Githinji, G., Gymrek, M., ... Vanderplas, J. T. (2018). Journal of Open Source Software (JOSS): Design and first-year review. *PeerJ Preprints*, 4, e147. doi: 10.7717/peerj-cs.147
- Solimando, A. G., Malerba, E., Leone, P., Prete, M., Terragna, C., Cavo, M., & Racanelli, V. (2022, September). Drug resistance in multiple myeloma: Soldiers and weapons in the bone marrow niche. *Frontiers in Oncology*, 12, 973836. Retrieved 2022-10-23, from <https://www.ncbi.nlm.nih.gov/pmc/articles/PMC9533079/> doi: 10.3389/fonc.2022.973836
- Stock, P., Bruckner, S., Winkler, S., Dollinger, M. M., & Christ, B. (2014, April). Human bone marrow mesenchymal stem cell-derived hepatocytes improve the mouse liver after acute acetaminophen intoxication by preventing progress of injury. *International journal of molecular sciences*, 15(4), 7004–7028. doi: 10.3390/ijms15047004
- Tam, P. P., & Beddington, R. S. (1987, January). The formation of mesodermal tissues in the mouse embryo during gastrulation and early organogenesis. *Development (Cambridge, England)*, 99(1), 109–126.
- Tanavalee, C., Luksanapruksa, P., & Singhatanadighe, W. (2016, June). Limitations of Using Microsoft Excel Version 2016 (MS Excel 2016) for Statistical Analysis for Medical Research. *Clinical Spine Surgery*, 29(5), 203. Retrieved 2024-03-11, from [https://journals.lww.com/jspinaldisorders/fulltext/2016/06000/limitations\\_of\\_using\\_microsoft\\_excel\\_version\\_2016.5.aspx](https://journals.lww.com/jspinaldisorders/fulltext/2016/06000/limitations_of_using_microsoft_excel_version_2016.5.aspx) doi: 10.1097/BSD.0000000000000382
- Team, T. P. D. (2020, February). *Pandas-dev/pandas: Pandas*. Zenodo. Retrieved from <https://doi.org/10.5281/zenodo.3509134> doi: 10.5281/zenodo.3509134
- Terpos, E., Ntanasis-Stathopoulos, I., Gavriatopoulou, M., & Dimopoulos, M. A. (2018, January). Pathogenesis of bone disease in multiple myeloma: From bench to bedside. *Blood Cancer Journal*, 8(1), 7. doi: 10.1038/s41408-017-0037-4
- Ullah, I., Subbarao, R. B., & Rho, G. J. (2015). Human mesenchymal stem cells - current trends and future prospective Bioscience Reports. doi: 10.1042/BSR20150025
- Urashima, M., Chauhan, D., Uchiyama, H., Freeman, G., & Anderson, K. (1995, April). CD40 ligand triggered interleukin-6 secretion in multiple myeloma. *Blood*, 85(7), 1903–1912. Retrieved 2021-02-01, from <https://ashpublications.org/blood/article/85/7/1903/123565/CD40-ligand-triggered-interleukin6-secretion-in> doi: 10.1182/blood.V85.7.1903.bloodjournal8571903
- Vallat, R. (2018, November). Pingouin: Statistics in Python. *Journal of Open Source Software*, 3(31), 1026. Re-

- trieved 2023-05-29, from <https://joss.theoj.org/papers/10.21105/joss.01026> doi: 10.21105/joss.01026
- van Rossum, G., Lehtosalo, J., & Langa, L. (2014). *PEP 484 – Type Hints / peps.python.org*. Retrieved 2024-03-08, from <https://peps.python.org/pep-0484/>
- Viguet-Carrin, S., Garnero, P., & Delmas, P. D. (2006, March). The role of collagen in bone strength. *Osteoporosis International*, 17(3), 319–336. Retrieved 2023-12-20, from <https://doi.org/10.1007/s00198-005-2035-9> doi: 10.1007/s00198-005-2035-9
- Waskom, M. L. (2021, April). Seaborn: Statistical data visualization. *Journal of Open Source Software*, 6(60), 3021. Retrieved 2023-03-26, from <https://joss.theoj.org/papers/10.21105/joss.03021> doi: 10.21105/joss.03021
- Weetall, M., Hugo, R., Maida, S., West, S., Wattanasin, S., Bouhel, R., ... Friedman, C. (2001, June). A Homogeneous Fluorometric Assay for Measuring Cell Adhesion to Immobilized Ligand Using V-Well Microtiter Plates. *Analytical Biochemistry*, 293(2), 277–287. Retrieved 2022-09-25, from <https://linkinghub.elsevier.com/retrieve/pii/S0003269701951401> doi: 10.1006/abio.2001.5140
- Wickham, H. (2014, September). Tidy Data. *Journal of Statistical Software*, 59, 1–23. Retrieved 2023-11-15, from <https://doi.org/10.18637/jss.v059.i10> doi: 10.18637/jss.v059.i10
- Wilkins, A., Kemp, K., Ginty, M., Hares, K., Mallam, E., & Scolding, N. (2009, July). Human bone marrow-derived mesenchymal stem cells secrete brain-derived neurotrophic factor which promotes neuronal survival in vitro. *Stem cell research*, 3(1), 63–70. doi: 10.1016/j.scr.2009.02.006
- Wilkinson, M. D., Dumontier, M., Aalbersberg, I. J., Appleton, G., Axton, M., Baak, A., ... Mons, B. (2016, March). The FAIR Guiding Principles for scientific data management and stewardship. *Scientific Data*, 3(1), 160018. Retrieved 2024-03-18, from <https://www.nature.com/articles/sdata201618> doi: 10.1038/sdata.2016.18
- Xu, W., Zhang, X., Qian, H., Zhu, W., Sun, X., Hu, J., ... Chen, Y. (2004, July). Mesenchymal stem cells from adult human bone marrow differentiate into a cardiomyocyte phenotype in vitro. *Experimental biology and medicine (Maywood, N.J.)*, 229(7), 623–631.
- Yang, A., Troup, M., & Ho, J. W. (2017, July). Scalability and Validation of Big Data Bioinformatics Software. *Computational and Structural Biotechnology Journal*, 15, 379–386. Retrieved 2024-03-07, from <https://www.ncbi.nlm.nih.gov/pmc/articles/PMC5537105/> doi: 10.1016/j.csbj.2017.07.002
- Zeissig, M. N., Zannettino, A. C. W., & Vandyke, K. (2020, December). Tumour Dissemination in Multiple Myeloma Disease Progression and Relapse: A Potential Therapeutic Target in High-Risk Myeloma. *Cancers*, 12(12). Retrieved 2021-02-03, from <https://www.ncbi.nlm.nih.gov/pmc/articles/PMC7761917/> doi: 10.3390/cancers12123643
- Zerbino, D. R., Achuthan, P., Akanni, W., Amode, M. R., Barrell, D., Bhai, J., ... Flicek, P. (2018, January). Ensembl 2018. *Nucleic Acids Research*, 46(D1), D754-D761. Retrieved 2023-05-27, from <https://doi.org/10.1093/nar/gkx1098> doi: 10.1093/nar/gkx1098
- Zhou, Y., Zhou, B., Pache, L., Chang, M., Khodabakhshi, A. H., Tanaseichuk, O., ... Chanda, S. K. (2019, April). Metascape provides a biologist-oriented resource for the analysis of systems-level datasets. *Nature Communications*, 10(1), 1523. Retrieved 2023-02-09, from <https://www.nature.com/articles/s41467-019-09234-6> doi: 10.1038/s41467-019-09234-6

# Appendices

## A Supplementary Data & Methods

### A.1 Figures

## A.2 Tables

### A.3 Materials & Methods

## B Documentation of `plotastic`